InP-based evanescently coupled high-responsivity photodiodes with extremely low dark current density integrated diluted waveguide at 1550 nm*

Zuo Yu-Hua(左玉华)†, Cao Quan(曹 权), Zhang Yun(张 云), Zhang Ling-Zi(张岭梓), Guo Jian-Chuan(郭剑川), Xue Chun-Lai(薛春来), Cheng Bu-Wen(成步文), and Wang Qi-Ming(王启明)

State Key Laboratory on Integrated Optoelectronics, Institute of Semiconductors, Chinese Academy of Sciences, Beijing 100083, *China*

(Received 20 January 2010; revised manuscript received 8 March 2010)

In this paper, we have demonstrated a high performance waveguide photodiode integrated diluted waveguide serving as a fibre-to-waveguide coupler to achieve high coupling efficiency. High responsivity (> 1 A/W), high saturation power (> 45 mA) in the static state and extremely low dark current density (0.04 pA/μm^2) with 3 dB bandwidth at 13.4 GHz have been achieved.

Keywords: high responsivity, diluted waveguide, evanescent coupling, waveguide photodiode

PACS: 85.60.Dw, 42.81.Qb, 73.40.Kp **DOI:** 10.1088/1674-1056/20/1/018504

1. Introduction

In order to meet the pressing need for microwave and millimeter-wave photonic systems with photodetector (PD) performances of high-responsivity, high bandwidth and high power (3-H PD) simultaneously, many approaches have been demonstrated.[1−5] Generally speaking, according to the working principles of photodiodes, there are two ways to realise the 3-H PD. One is to enlarge the absorption volume of the photodiodes and distribute the photocurrents along edge-coupled PDs more uniformly, for example traveling-wave PDs, or waveguide PDs with a diluted waveguide.[6−8] For example, a 24 dBm output power and a 30 mA output current at 40 GHz were obtained with a diluted waveguide structure by Shi *et al.*[9] The other method is to reduce the space-charge effect of photo-generated carriers in the absorption region by designing creative energy band structures of PD epitaxial layers, such as uni-traveling carrier PDs (UTC-PDs) and doped absorption epitaxial layers. Recently, 20 mW output power of a UTC-PD was obtained at 100 GHz by NTT.[10] With a modified UTC-PD structure, 120 mA saturation current at 20 GHz and 22 mA saturation current at 50 GHz were obtained by Chtioui *et al.*[11] Using a partially doped absorption (PDA) structure, a 260 mA saturation current with 24 dBm output power was obtained at 6 GHz, while 700 mA saturation current was obtained at 300 MHz by Williams *et al.*[12]

Two major factors restrict photodiode output power: the space-charge effect[1,12−15] and the thermal effect.[15,16] For waveguide photodiodes, in which a tradeoff between responsivity and bandwidth is realised, two factors are responsible for restricting the potential applications of these structures.[15] The first restriction is the difficulty in designing the absorber to achieve uniform illumination over the absorber area. This is because nonuniform illumination will lead to nonuniform distribution of carriers, thereby enhancing the space-charge effect. The second restriction is the power limitation of the input facet. A high power density of the input facet will cause heat damage to the facet before the photogenerated current reaches saturation.

Our evanescent coupling waveguide photodiodes, however, can solve the two problems satisfactorily. By using the diluted waveguide and two optical matching layers, the illumination of the absorber can be uniform and the power density of the input facet can be diluted to a relatively low level. As a result, a saturation current higher than 45 mA is obtained. At the same time, the input optical power can be higher than 80 mW, which is useful in radio-over-fibre (ROF) systems. In addition, a responsivity of 1.05 A/W and 0.04 pA/μm^2 dark current density, and 13.4 GHz

*Project supported by the National High Technology Research and Development Program of China (Grant No. 2006CB302802).
†Corresponding author. E-mail: yhzuo@red.semi.ac.cn
© 2011 Chinese Physical Society and IOP Publishing Ltd

bandwidth are obtained. That is the highest responsivity reported so far.

In this paper, the design and the fabrication are described, and the optoelectronic characteristics are also presented.

2. Design and fabrication

Highly efficient coupling of a fibre to a waveguide is always important for waveguide photodetectors. Recently, a diluted waveguide has been used to evanescently couple the light mode from a fibre to a waveguide.[6,7,17] Figure 1(a) shows a schematic of our evanescently coupled photodiode (ECPD) in which a diluted waveguide and two optical matching layers are used.

The design and analysis of the diluted waveguide and two optical matching layers were summarised in Refs. [18] and [19]. The 30 μm long input waveguide was comprised of a stack of 10-period un-doped 120 nm InP/80 nm InGaAsP (1.05-μm band gap) multiple layers, a 420 nm thick n^+-doped $Q1.05$ coupling layer, and a 100 nm thick undoped $Q1.2$ interlayer. The absorption structure was composed of a 400 nm thick undoped $Q1.66$ InGaAs absorption layer, a 100 nm thick undoped $Q1.4$ InGaAsP diffusion stop layer, and a 150 nm thick p^+-doped layer. The simulation shows that the diluted waveguide has a polarisation dependence as low as 0.1 dB. And the fibre-to-waveguide coupling efficiency η_c is as high as 92%. Also, the two optical matching layers make the absorption more uniform and efficient according to the optical matching theory proposed by Deri and Wada.[20]

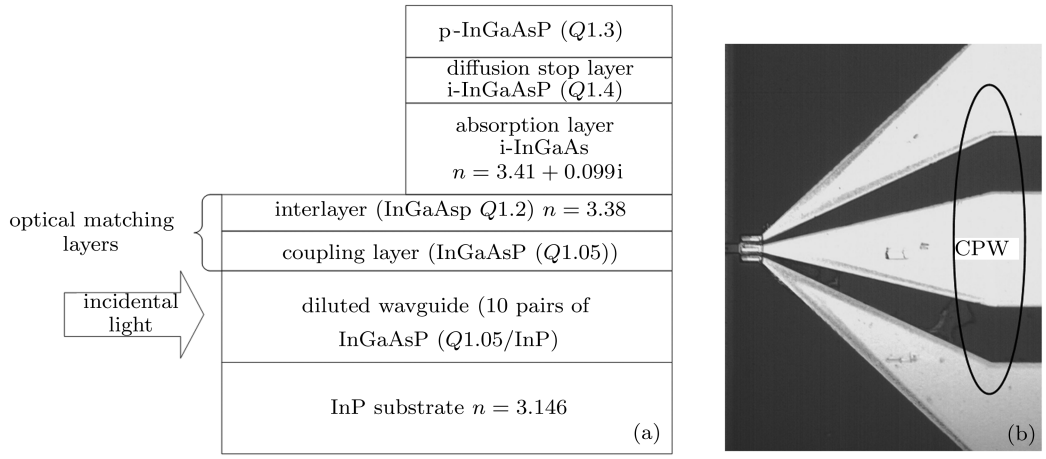


Fig. 1. (a) Conceptual schematic cross section of the ECPD, and (b) top view of the fabricated device.

The device was fabricated using standard photolithography, metallisation and dry etching processes. Six steps of photolithography were used to determine the waveguide structure that comprises of the active region, the p electrode, the n electrode, the dig hole and the electrical pads. The waveguide structure of our ECPD was determined by the dry etching process using SiO_2 as a passive mask. SiO_2 was also used for passivation. The co-planar waveguide (CPW) transmission lines, formed by the Ti/Al/Ti/Au interconnect metal, was deposited by magnetron sputtering, which was expected to give low series resistance and good adhesion. Then the device was precisely cleaved to obtain a smooth facet of the waveguide, and an anti-reflective (AR) coating was deposited on the facet to reduce the reflection loss of the passive waveguide. In this way, the ECPD was fabricated as shown in Fig. 1(b).

3. Measurement and discussion

The frequency response and the saturation current of the fabricated ECPD were measured and the measurement system is shown in Fig. 2.

A tunable semiconductor laser was employed as a light source for dc photocurrent measurement, when the central wavelength of this laser was fixed at 1550 nm.

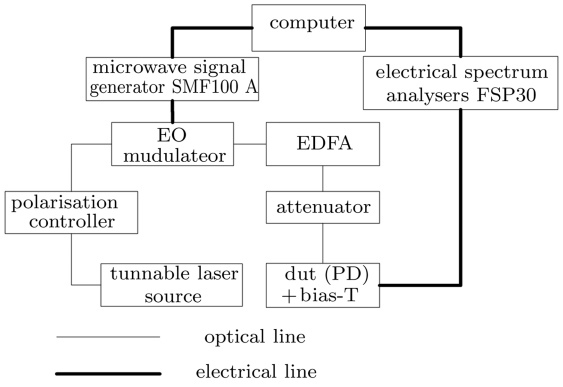


Fig. 2. Measurement system of ECPD.

A high responsivity of a diode with an absorption area of 12 μm×30 μm is obtained. The relatively high responsivity confirms the high fibre-to-waveguide coupling efficiency of the diluted waveguide and the high optical power transfer efficiency from the diluted waveguide to the absorption layer. This is the highest responsivity reported so far. We believe that this is attributed to the relatively long absorption region. However, the large volume of the absorption region can lead to a decrease in the resistor–capacitor (RC) limited frequency response. The dark current was also measured under the static condition as shown in Fig. 3. The I–V characteristic curve of the 12 μm wide and 30 μm long diode was tested. The dark current was 11.5 pA when no bias voltage was applied. At −1 V, the dark current increased to only 9.9 nA. The low dark current density, (< 0.04 pA/μm^2), can be attributed to the high quality of the epitaxial layer growth and good passivation with the thick SiO_2 layer in the fabrication process.

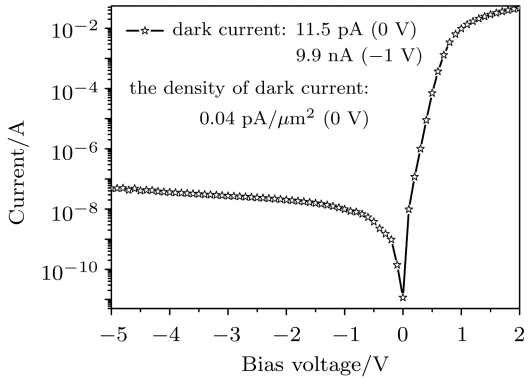


Fig. 3. Measured dark currents at bias voltages of 0 V and −1 V.

The measured frequency response of our device (12 μm×30 μm) is shown in Fig. 4. The device with an active area of 360 μm^2 was measured under a fixed dc bias voltage (−3 V), and showed an $f_{3\mathrm{dB}}$ bandwidth of about 13.4 GHz. The influences of microwave probe, radio-frequency (RF) cable, and RF bias tee on measured frequency response were removed using the RF correction technique and a vector network analyser.

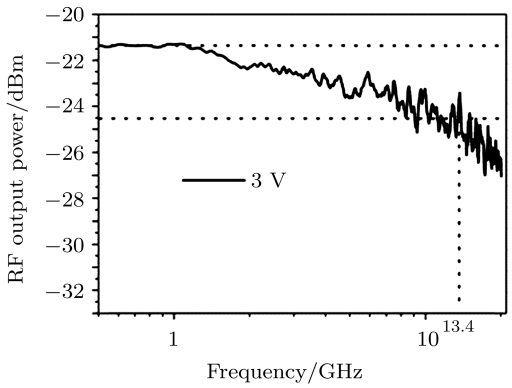


Fig. 4. Measured frequency response of the ECPD under a fixed dc bias voltage (−3 V).

The calculated bandwidth of the device is limited to about 21 GHz (−3 V), which is much higher than the experimental result. There are two reasons for the decrease in the experimental result for $f_{3\mathrm{dB}}$. The first is the ohmic contact resistance up to 30 Ω brought about by the fabrication process, which increased microwave reflections and thus reduced the high-frequency characteristics due to the impedance mismatch. The second reason is the neglected parasitic resistance and capacitance in the calculation, which would reduce the device high-frequency characteristics in a real situation.

The saturation characteristics of the ECPD are shown in Figs. 5 and 6. The curves for static optical current versus incident optical power at different reverse bias voltages were measured without an operating frequency. As shown in the two figures, the device with larger geometry has a higher static optical current. This is because without applying an operation frequency, the RF power generation will be unaffected by the RC bandwidth limitation and related to the space-charge effect.[15] Generally speaking, devices with larger geometries have lower densities of photogenerated carriers and fewer space charge shielding effects, so they have better saturation behaviour. The highest static saturation current (45 mA) was observed at reverse voltages of 1 V and 3 V in the device with 40 μm length. In addition, as shown in Figs. 5 and 6, our ECPD could stand up to a high incident optical power of more than 80 mw, which reveals the great advantage of the ROF system.[1,4]

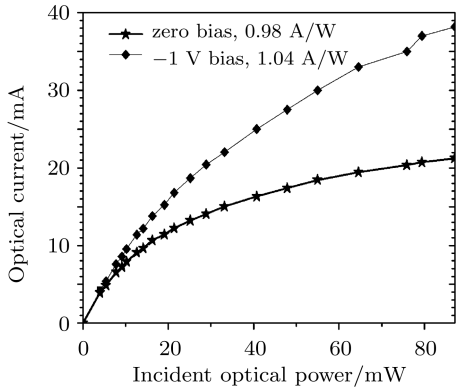


Fig. 5. Curves for static optical current versus incident optical power of 30 μm length devices at reverse bias voltages of 0 V and 1 V.

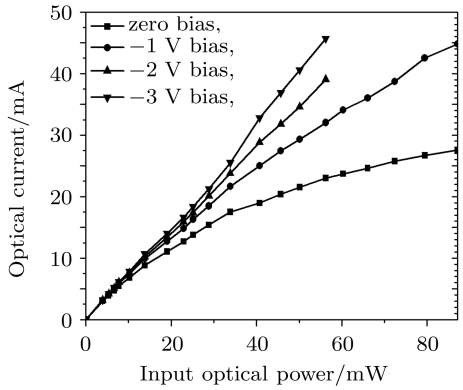


Fig. 6. Curves for static optical current versus incident optical power of 40 μm length devices at reverse bias voltages of 0 V, 1 V.

We found the interesting phenomenon that the optical current trend versus incident optical power showed a good linearity until the diodes were damaged for the 40 μm long devices. This phenomenon was especially significant when a high reverse voltage was applied. This may imply that the nonlinear effect in the space charge region is not a main limiting factor in the high current output situation.[4,12,15] The diodes were burned down due to the heat generated by the high current level before the nonlinear effect appeared. So the thermal limitations will be improved in future designs to provide an overall optimisation scheme for achieving high currents.[5]

4. Conclusion

By utilising a diluted waveguide and two optical matching layers, an ECPD with high coupling efficiency up to 93% and low polarisation dependence (< 0.7 dB) was fabricated. Our ECPD shows a responsivity of up to 1.05 A/W, a bandwidth of 13.4 GHz, a 45 mA static optical current and an extremely low dark current density (0.04 pA/μm^2). Our ECPD also shows an advantage in standing up to a high incident light power, which can be applied to the ROF system. There is still much scope for optimising the overall performance. The bandwidth can be greatly improved by using a small absorption area and producing a smaller ohmic resistance due to the reduction in RC bandwidth limitation. In addition, the saturation output current can be improved by using the UTC structure owing to the reduction of the space charge effect.

References

[1] Williams K J, Tulchinsky D A and Campbell J C 2007 *2007 International Topical Meeting on Microwave Photonics* The Fairmont Empress Victoria, BC, Canada, Oct. 2–5 2007 p9

[2] Chtioui M, Enard A, Carpentier D, Bernard S, Rousseau B, Lelarge F, Porrimereau F and Achouche M 2008 *IEEE Photonic Tech. Lett.* **20** 202

[3] Seeds A J and Williams K J 2006 *J. Lightwave Technol.* **24** 4628

[4] Nagatsuma T, Ito H and Ishibashi T 2009 *Laser Photonics Rev.* **3** 123

[5] Nagatsuka T, Itakura S, Sakai K and Hirano Y 2008 *2008 Joint Conference of the Opto-Electronics and Communications Conference and the Australian Conference on Optical Fibre Technology* Sydney 7–10 July 2008 **1,2** p277

[6] Wu Y S, Shi J W, Wu J Y, Huang F H, Chan Y J, Huang Y L and Xuan R 2005 *IEEE Photonic Tech. Lett.* **17** 878

[7] Wu Y S, Shi J W, Chiu P H and Lin W 2007 *IEEE Photonic Tech. Lett.* **19** 1682

[8] Jasmin S, Vodjdani N, Renaud J C and Enard A 1997 *IEEE T. Microw. Theory* **45** 1337

[9] Shi J W, Wu Y S, Wu C Y, Chiu P H and Hong C C 2005 *IEEE Photonic Tech. Lett.* **17** 1929

[10] Ito H, Nagatsuma T, Hirata A, Minotani T, Sasaki A, Hirota Y and Ishibashi T 2003 *IEEE P-Optoelectron.* **150** 138

[11] Chtioui M, Enard A, Carpentier D, Bernard S, Rousseau B, Lelarge F, Pommereau F and Achouche M 2008 *IEEE Photonic Tech. Lett.* **20** 1163

[12] Williams K J, Tulchinsky D A, Boos J B, Park D, Goetz P G and Rabinovich W S 2006 *2006 International Topical Meeting on Microwaves Photonics* Grenoble, France 3–6 Oct. 2006 p93

[13] Williams K J, Esman R D and Dagenais M 1994 *IEEE Photonic Tech. Lett.* **6** 639

[14] Liu P L, Williams K J, Frankel M Y and Esman R D 1999 *IEEE T. Microw. Theory* **47** 1297

[15] Williams K J and Esman R D 1999 *J. Lightwave Technol.* **17** 1443

[16] Islam M S, Nespola A, Yeahia M, Wu M C, Sivco D L and Cho A Y 2000 *Leos 2000 — IEEE Annual Meeting Conference Proceedings* Rio Grande, Puerto Rico 13–16 Nov. 2000 **1,2** p82

[17] Zhang Y X, Liao Z Y and Wang W 2009 *Chin. Phys.* B **18** 2393

[18] Zhang Y, Zuo Y H, Guo J C, Ding W C, Cheng B W, Yu J Z and Wang Q M 2009 *Chin. Phys.* B **18** 225

[19] Zhang Y, Guo J C, Ding W C, Cheng B W, Yu J Z and Wang Q M 2008 *J. Semiconductors* **29** 555

[20] Hawkins R J, Deri R J and Wada O 1991 *Opt. Lett.* **16** 470